



# RESEARCH MEMORANDUM

for the

Bureau of Aeronautics, Department of the Navy

FLIGHT DETERMINATION OF THE LOW-LIFT DRAG AND LONGITUDINAL

STABILITY OF A  $\frac{1}{10}$  - SCALE ROCKET-POWERED MODEL

OF THE DOUGLAS XF4D-1 AIRPLANE AT

MACH NUMBERS FROM 0.7 TO 1.4

TED NO. NACA DE 349

By Grady L. Mitcham, Willard S. Blanchard, Jr.,  
and Earl C. Hastings, Jr.

Langley Aeronautical Laboratory  
Langley Field, Va.

CLASSIFIED DOCUMENT

This material contains information affecting the National Defense of the United States within the meaning of the espionage laws, Title 18, U.S.C., Secs. 793 and 794, the transmission or revelation of which in any manner to unauthorized person is prohibited by law.

## NATIONAL ADVISORY COMMITTEE FOR AERONAUTICS

WASHINGTON

*Handwritten:* 8/9/68  
68H  
WSS  
ECB

*Handwritten:* 3/9/90  
This material has been removed  
E7 10958 dated 4-17-95  
ACM

UNCLASSIFIED

NACA RM SL51L07



UNCLASSIFIED

NATIONAL ADVISORY COMMITTEE FOR AERONAUTICS

RESEARCH MEMORANDUM

for the

Bureau of Aeronautics, Department of the Navy

FLIGHT DETERMINATION OF THE LOW-LIFT DRAG AND LONGITUDINAL

STABILITY OF A  $\frac{1}{10}$  - SCALE ROCKET-POWERED MODEL

OF THE DOUGLAS XF<sup>4</sup>D-1 AIRPLANE AT

MACH NUMBERS FROM 0.7 TO 1.4

TED NO. NACA DE 349

By Grady L. Mitcham, Willard S. Blanchard, Jr.,  
and Earl C. Hastings, Jr.

SUMMARY

A flight investigation has been made to determine the drag and longitudinal stability of a  $\frac{1}{10}$  - scale model of the Douglas XF<sup>4</sup>D-1 airplane from Mach numbers 0.7 to 1.4 at lift coefficients near zero.

The drag rise occurred near  $M = 0.95$ . The external drag coefficient was a constant value of about 0.012 at subsonic speeds up to the point of drag rise where it increased abruptly to a value of 0.030 at  $M = 1.0$  followed by a more gradual increase to a value of 0.038 at  $M = 1.25$ . The model indicated that, at 35,000 feet and a level-flight free-stream Mach number of 1.0, the drag of the full-scale airplane would exceed the thrust available from an XJ40-WE-8 engine with afterburning. The transonic trim change was small. The aerodynamic center moved gradually from the most forward location of 21.0-percent mean aerodynamic chord at  $M = 0.9$  to the most rearward location of 40-percent mean aerodynamic chord at  $M = 1.25$ . The damping in pitch was low.

INTRODUCTION

An investigation of the drag and longitudinal trim characteristics of  $\frac{1}{10}$  - scale rocket-powered models of the Douglas XF<sup>4</sup>D-1 airplane at

~~CONFIDENTIAL~~

UNCLASSIFIED

transonic and low supersonic speeds is being conducted by the Langley Pilotless Aircraft Research Division at the request of the Bureau of Aeronautics, Department of the Navy.

The Douglas XF4D-1 is a jet-propelled, single-place, low-aspect-ratio, swept-wing, tailless, interceptor-type airplane designed to fly at low supersonic speeds. The over-all investigation includes the effects of various combinations of external stores and rocket packages on the drag and longitudinal trim.

The primary purpose of the test reported herein was to determine the drag at low lift coefficients for the airplane in the clean condition. In addition to these data, stability derivatives are also presented since it was possible to analyze the short-period oscillations induced by booster separation and the trim change near a Mach number of 1.0.

#### SYMBOLS

|           |   |
|-----------|---|
| M         | Mach number   |
| R         | Reynolds number   |
| V         | velocity, feet per second   |
| p         | static pressure, pounds per square foot   |
| H         | total pressure, pounds per square foot  |
| q         | dynamic pressure, pounds per square foot  |
| $\rho$    | density of air, slugs per cubic foot  |
| A         | duct area, square feet  |
| m         | mass flow through duct, $(\rho_{\text{duct}} V_{\text{duct}} A_{\text{duct}})$ , slugs per second   |
| $m_0$     | mass of air flowing through a stream tube of area equal to the inlet-cowl area under free-stream conditions, $(\rho_0 V_0 A_{\text{inlet}})$ , slugs per second |
| S         | wing area of model, square feet   |
| $\bar{c}$ | mean aerodynamic chord, feet  |
| W         | weight of model, pounds   |

|                                     |   |
|-------------------------------------|---|
| $a_l/g$                             | longitudinal accelerometer reading  |
| $a_n/g$                             | normal accelerometer reading  |
| $g$                                 | acceleration due to gravity, 32.2 feet per second per second  |
| $C_c$                               | chord-force coefficient $\left(\frac{a_l}{g} \frac{W}{q_0 S}\right)$  |
| $C_N$                               | normal-force coefficient $\left(\frac{a_n}{g} \frac{W}{q_0 S}\right)$   |
| $C_D$                               | drag coefficient (Drag/ $q_0 S$ )   |
| $C_L$                               | lift coefficient (Lift/ $q_0 S$ )   |
| $T_c'$                              | thrust coefficient (Thrust/ $q_0 S$ )   |
| $\frac{P_{\text{base}} - P_0}{q_0}$ | base-pressure coefficient of choking cup  |
| $C_{N_{\text{trim}}}$               | trim-normal-force coefficient   |
| $C_{m_\alpha}$                      | rate of change of pitching-moment coefficient about center of gravity with respect to angle of attack, per degree |
| $I_y$                               | moment of inertia in pitch, slug-feet <sup>2</sup>  |
| $P$                                 | period of short-period longitudinal oscillation, seconds  |
| $T_{1/2}$                           | time required for short-period longitudinal oscillation to damp to 1/2 amplitude, seconds                         |
| $\dot{\theta}$                      | rate of change of pitch angle with time, radians per second<br>$\left(\frac{d\theta}{dt}\right)$                  |
| $\dot{\alpha}$                      | rate of change of angle of attack with time, radians per second<br>$\left(\frac{d\alpha}{dt}\right)$              |

$$C_{m\dot{\theta}} = \frac{\partial C_m}{\partial \left(\frac{d\theta}{dt}\right)}$$

$$C_{m\dot{\alpha}} = \frac{\partial C_m}{\partial \left(\frac{d\alpha}{dt}\right)}$$

## Subscripts:

|       |                     |
|-------|---------------------|
| o     | free stream         |
| inlet | duct inlet          |
| exit  | duct exit           |
| base  | base of choking cup |

## MODELS AND APPARATUS

## Models

A three-view drawing of the  $\frac{1}{10}$ -scale model used in the present investigation is shown in figure 1. Photographs of the model are shown as figures 2 to 5. Table 1 gives the dimensional and mass characteristics. The model was constructed essentially of wood with aluminum inserts and castings. The elevon deflection was fixed, trailing edge up  $0.3^\circ$  prior to the flight test, and the trimmer was built integral with the model and was not deflected.

A cup designed to give choking at the exit was installed in the model. This installation was made in order that an accurate determination of internal drag could be made with a minimum number of pressure measurements and to duplicate inlet Mach number of the full-scale airplane at  $M = 1.4$ . A sketch of the choking-cup installation is shown in figure 1 and a photograph is shown as figure 4. The location of the total-pressure tube and the static-pressure orifice in one of the ducts is shown in figure 1. A plot of duct cross-sectional area from the inlet to the exit is shown in figure 6.

Prior to flight testing, the model was suspended by shock cords and shaken in the pitch plane with an electromagnetic shaker at frequencies up to 400 cycles per second. A fundamental frequency of 83 cycles per second (first bending) was observed from the telemeter record taken during the ground tests. As expected, only the normal acceleration channel showed any frequency response in the ground tests. Resonance occurred at 83, 180, and 240 cycles per second.

The model was boosted to  $M = 1.4$  by a solid-fuel, 6-inch-diameter Deacon rocket motor which produces an average thrust of 6500 pounds for approximately 3.1 seconds. The model contained no internal-rocket-sustainer motor.

Launching was accomplished from the zero-length launcher seen in figure 5.

### Apparatus

The flight time history of the model was transmitted and recorded by a telemeter system which gave eight continuous channels of information. The information measured during this flight test consisted of normal, longitudinal, and transverse acceleration, free-stream total pressure, inlet total pressure, inlet static pressure, exit static pressure, and choking-cup base pressure. A radiosonde released at time of firing was used to obtain free-stream temperature and static pressure. Ground equipment consisting of a CW Doppler radar unit and a radar tracking unit was used to determine model velocity and position in space.

### METHOD OF ANALYSIS

All data reported herein were obtained during the decelerating portion of the flight following separation of the model from the booster.

Drag.- Since the model flew at virtually zero normal-force coefficient throughout the test speed range, the total-drag coefficient was assumed equal to the chord-force coefficient. The values of drag coefficient were ascertained by two independent methods. The first method involved the use of a longitudinal accelerometer mounted in the model and the second method involved differentiation with respect to time of the velocity along the flight path as determined from Doppler radar and tracking radar.

The choking cup (figs. 1 and 4) was designed to maintain a Mach number of 0.32 at the duct inlets and a Mach number of 1.00 at the exit at supersonic speeds. With these conditions known, mass flow and internal drag can be determined using exit static-pressure and free-stream conditions (see reference 1). Internal drag was determined by means of the relationship

$$C_{D_{\text{internal}}} = \frac{1}{q_0 S} \left[ m(V_0 - V_{\text{exit}}) - A_{\text{exit}}(P_{\text{exit}} - P_0) \right]$$

Base drag was determined from

$$C_{D_{\text{base}}} = \frac{-(P_{\text{base}} - P_0)A_{\text{base}}}{q_0 S}$$

External drag was obtained by subtracting internal and base drag from total drag.

$$C_{D_{\text{external}}} = C_{D_{\text{total}}} - C_{D_{\text{internal}}} - C_{D_{\text{base}}}$$

Lift.- Since the lift coefficient throughout the flight was very low, lift was determined from the relationship

$$C_L = C_N = \frac{(a_n/g)W}{qS}$$

where the term  $(a_n/g)$  was obtained from the telemeter signal transmitted by the normal accelerometer mounted in the model.

Static longitudinal stability.- Oscillations in pitch were excited by several disturbances which occurred during the flight. The first oscillation was caused by the sudden change in trim when the model and booster separated; the second was the result of the transonic trim change; the third was apparently caused by a gust which occurred at a Mach number of about 0.85. These oscillations were analyzed for the determination of the period of the short-period longitudinal oscillation. Static longitudinal stability was then obtained as follows:

$$\frac{dC_m}{d\alpha} = C_{m\alpha} = - \frac{4\pi^2 I_y}{P^2 q_0 S \bar{c}}$$

$$\frac{dC_m}{dC_L} = C_{mC_L} = \frac{C_{m\alpha}}{C_{L\alpha}}$$

where  $C_{L\alpha}$  was obtained from reference 2.

Damping in pitch.- Where possible, the pitch oscillations were analyzed in an attempt to ascertain  $T_{1/2}$ . It is felt, however, that only the value obtained immediately after separation (highest Mach number) is reliable quantitatively; the other two values obtained serve only as qualitative indications that damping was low, since the amplitudes of the oscillations were so small that accurate determination of  $T_{1/2}$  was impossible. Total damping was determined from the relationship

$$C_m \frac{\partial \bar{c}}{2V} + C_m \frac{\partial \bar{c}}{2V} = \frac{-8I_y}{\rho V S \bar{c}^2} \left( \frac{0.693}{T_{1/2}} - \frac{C_{L\alpha} \rho V S g}{4W} \right)$$

More complete discussions of the methods used in reducing data of this type are given in references 3 and 4.

## PRECISION OF DATA

The estimated maximum errors in some of the data are presented in the following table:

|                    | Supersonic   | Subsonic     |
|--------------------|--------------|--------------|
| $C_{D_{total}}$    | $\pm 0.0005$ | $\pm 0.001$  |
| $C_{D_{internal}}$ | $\pm 0.0001$ | -----        |
| $C_{D_{base}}$     | $\pm 0.0001$ | $\pm 0.0002$ |
| $C_{D_{external}}$ | $\pm 0.0007$ | -----        |
| $m/m_0$            | $\pm 0.04$   | -----        |
| $H_{inlet}/H_0$    | $\pm 0.04$   | $\pm 0.08$   |
| M                  | $\pm 0.005$  | $\pm 0.01$   |

## RESULTS AND DISCUSSION

The variation of Reynolds number with Mach number is shown in figure 7. The center of gravity of the model was located 16.7 percent behind the leading edge of the mean aerodynamic chord throughout this investigation.

## Trim Lift Coefficient

The range of trim-lift coefficient of this flight investigation is shown as a function of Mach number in figure 8. Since the elevons were fixed at a very small deflection ( $-0.3^\circ$ ), figure 8 represents the longitudinal trim characteristics of the airplane in the clean condition. The transonic trim change was small amounting to only  $\pm 0.025$  change in lift coefficient between  $M = 0.95$  and  $M = 1.02$ .

## Buffet and Flutter

As mentioned previously, resonant frequencies of the model were determined prior to the flight test. Analysis of the telemeter records of the flight, however, indicated that no buffet or flutter was present during the flight.

## Drag

The base-pressure coefficient of the choking cup is presented in figure 9. The results show that the base pressure decreases from a positive pressure at subsonic speeds to a negative pressure near  $M = 1.0$  and remains negative at supersonic speeds. This phenomenon has been observed on other models with comparable boattail angles at the base (reference 5). This base pressure converted to base-drag coefficient is shown in figure 10. As might be expected, the base drag represents a small part of the total drag.

The internal-drag coefficient (fig. 10) was roughly constant at 0.0009 above  $M = 1.0$ . Values of internal-drag coefficient at subsonic speeds were not obtained since it was not possible to obtain a Mach number of 1.0 at the duct exit.

A summary of the drag data is given in figure 11. The total drag coefficient is nearly constant at a value of 0.012 from  $M = 0.72$  to  $M = 0.95$ , the point at which the drag rise begins, followed by an abrupt increase to a value of 0.030 at  $M = 1.0$ , then a more gradual increase to a value of 0.039 at  $M = 1.25$ . Values of external-drag coefficient obtained from unpublished wind-tunnel data for the same configuration are shown plotted in figure 11. As indicated in the preceding discussion and figures, the contributions of base drag and internal drag to the over-all drag are small. These two increments of drag were subtracted from the total drag coefficient to give the external-drag coefficient as presented in figure 11. Assuming that the internal-drag coefficient below  $M = 1.0$  is equal to the internal-drag coefficient above  $M = 1.0$ , the values of total and external-drag coefficients are virtually the same at subsonic speeds. At supersonic speeds the external drag is smaller than the total drag by an increment in drag coefficient of about 0.0012. Mass-flow ratios for this test and the unpublished wind-tunnel test are shown in figure 12. As might be expected, the higher mass-flow ratio corresponds to lower external drag.

Also shown in figure 11 is estimated thrust coefficient of the XJ40-WE-8 engine with afterburning at an altitude of 35,000 feet. The thrust coefficient intersects the zero lift-drag coefficient at  $M = 1.0$ ; therefore, when drag due to lift is considered the maximum level-flight Mach number will be less than 1.0.

Two factors possibly contributing to the high drag of this configuration are the sharp boattailing of the fuselage and the duct inlets. The effect of comparable degrees of boattailing on the drag of bodies of revolution is shown in reference 6. Reference 7 indicates that this type of inlet tends toward a drag coefficient which increases with Mach number well into the supersonic range.

#### Relative Mass Flow

The variation of relative mass flow with Mach number is shown in figure 12. These values of relative mass flow were controlled by the choking cup located in the rear of the model.

#### Total Pressure Recovery

The total pressure in the duct was measured at station 24.30 as shown in figure 1. The measurements at this station were made to determine the existence of instability of flow from two ducts discharging into a common duct. Mass flow based on the total-pressure and static-pressure tubes in the duct indicated no flow instability. The total-pressure recovery measured by the total-pressure tube at station 24.30 is presented as a function of Mach number in figure 13. At the higher Mach numbers of the test the losses are considerably larger than those experienced through a normal shock. These losses are probably the result of flow separation in the vicinity of the duct inlet.

#### Static Longitudinal Stability

As stated in the introduction, the primary purpose of this investigation was to determine drag at low lift coefficients. However, as a result of several disturbances in pitch which occurred during the flight, it was possible to measure the period of the short-period longitudinal oscillations. These values are presented in figure 14. The values for period were used to calculate the static longitudinal stability parameter  $C_{m\alpha}$  which is shown in figure 15. The center-of-gravity location of the model (16.7 percent  $\bar{c}$ ) was forward of the center-of-gravity location quoted for the full-scale airplane in reference 2.

The values for slope of the lift curve given in reference 2 were used in the calculation of the aerodynamic-center location which is presented in figure 16. The aerodynamic center moves gradually from the most forward location of 21.0-percent mean aerodynamic chord at  $M = 0.9$  to the most rearward location at 40-percent mean aerodynamic chord at  $M = 1.25$ .

### Damping in Pitch

The short-period longitudinal oscillations which occurred during the flight (see "Method of Analysis") were analyzed to obtain a limited amount of damping data. The maximum magnitude of the oscillations decreased with decreasing Mach number, thereby decreasing the accuracy of  $T_{1/2}$ , as shown in figure 17. Values of total damping factor  $C_{m\dot{\theta}} + C_{m\dot{\alpha}}$  based on these values of  $T_{1/2}$  are shown in figure 18. Although these values are of limited accuracy, as seen in figure 18, they do indicate that damping in pitch at low lift coefficients is low and that further investigation is warranted.

### CONCLUSIONS

From an analysis of the results of the flight test of a  $\frac{1}{10}$ -scale rocket-powered model of the Douglas XF4D-1 airplane from  $M = 0.7$  to  $M = 1.4$  the following conclusions are indicated:

1. The external drag coefficient was approximately a constant value of 0.012 from  $M = 0.75$  to  $M = 0.95$ , the point at which the drag rise began, then increased abruptly to a value of 0.030 at  $M = 1.0$  followed by a more gradual increase to a value of 0.038 at  $M = 1.25$ .
2. At 35,000 feet, maximum level-flight Mach number of the full-scale airplane will be less than 1.0 when the XJ40-WE-8 engine with afterburning is used.
3. The transonic trim change was small.
4. The aerodynamic center moved gradually from the most forward location of 21.0-percent mean aerodynamic chord at  $M = 0.9$  to the most rearward location of 40-percent mean aerodynamic chord at  $M = 1.25$ .

5. The damping in pitch at lift coefficients near zero was low.

Langley Aeronautical Laboratory  
National Advisory Committee for Aeronautics  
Langley Field, Va.

*Grady L. Mitcham*

Grady L. Mitcham  
Aeronautical Engineer

*Willard S. Blanchard Jr.*

Willard S. Blanchard, Jr. <sup>by GLM</sup>  
Aeronautical Research Scientist

*Earl C. Hastings Jr.* <sup>by GLM</sup>

Earl C. Hastings, Jr.  
Aeronautical Research Intern

Approved:

*Joseph A. Shortal*

Joseph A. Shortal  
Chief of Pilotless Aircraft Research Division

mjw

~~CONFIDENTIAL~~

UNCLASSIFIED

## REFERENCES

1. Faget, Maxime A., Watson, Raymond S., and Bartlett, Walter A., Jr.: Free-Jet Tests of a 6.5-Inch-Diameter Ram-Jet Engine at Mach Numbers of 1.81 and 2.00. NACA RM L50L06, 1951.
2. Stability and Control Characteristics of Douglas Model XF4D-1 Part II. Transonic Flying Qualities. Douglas Report ES 15304.
3. Mitcham, Grady L., Stevens, Joseph E., and Norris, Harry P.: Aerodynamic Characteristics and Flying Qualities of a Tailless Triangular-Wing Airplane Configuration As Obtained from Flights of Rocket Propelled Models at Transonic and Low Supersonic Speeds. NACA RM L9L07, 1950.
4. Gillis, Clarence L., Peck, Robert F., and Vitale, A. James: Preliminary Results from a Free-Flight Investigation at Transonic and Supersonic Speeds of the Longitudinal Stability and Control Characteristics of an Airplane Configuration with a Thin Straight Wing of Aspect Ratio 3. NACA RM L9K25a, 1950.
5. Katz, Ellis R., and Stoney, William E., Jr.: Base Pressures Measured on Several Parabolic-Arc Bodies of Revolution in Free Flight at Mach Numbers from 0.8 to 1.4 and at Large Reynolds Numbers. NACA RM L51F29, 1951.
6. Hart, Roger G., and Katz, Ellis R.: Flight Investigations at High-Subsonic, Transonic, and Supersonic Speeds to Determine Zero-Lift Drag of Fin-Stabilized Bodies of Revolution Having Fineness Ratios of 12.5, 8.91, and 6.04 and Varying Positions of Maximum Diameter. NACA RM L9I30, 1949.
7. Sears, Richard I., and Merlet, C. F.: Flight Determination of the Drag and Pressure Recovery of an NACA 1-40-250 Nose Inlet at Mach Numbers from 0.9 to 1.8. NACA RM L50L18, 1951.

TABLE I

PHYSICAL CHARACTERISTICS OF A  $\frac{1}{10}$  - SCALE MODEL OF XF4D-1 AIRPLANE

## Wing:

|   |                             |
|---|-----------------------------|
| Area (included), sq ft . . . . .                          | 5.57                        |
| Span, ft . . . . .  | 3.35                        |
| Aspect ratio . . . . .                                    | 2.01                        |
| Mean aerodynamic chord, ft . . . . .                      | 1.82                        |
| Sweepback of leading edge, deg . . . . .                  | 52.5                        |
| Dihedral (relative to mean thickness line), deg . . . . . | 0                           |
| Taper ratio (Tip chord/Root chord) . . . . .              | 0.33                        |
| Airfoil section at root . . . . .                         | NACA 0007-63/30-9.5° Mod.   |
| Airfoil section at tip . . . . .                          | NACA 0004.5-63/30-9.5° Mod. |

## Vertical tail:

|  |                       |
|--|-----------------------|
| Area (leading edge extended to center line), sq ft . . . . . | 0.48                  |
| Aspect ratio . . . . .                                       | 2.08                  |
| Height (above fuselage center line), ft . . . . .            | 1.00                  |
| Sweepback of leading edge, deg . . . . .                     | 33.4                  |
| Taper ratio (Tip chord/Root chord) . . . . .                 | 0.26                  |
| Airfoil section at root . . . . .                            | NACA 0008-63/30-9°    |
| Airfoil section at tip . . . . .                             | NACA 0006-63/30-6.45° |

## Elevon:

|                             |      |
|-----------------------------|------|
| Area (one), sq ft . . . . . | 0.23 |
| Span (one), ft . . . . .    | 1.12 |
| Chord, ft . . . . .         | 0.22 |

## Weight and balance:

|  |       |
|--|-------|
| Weight, lb . . . . .                                       | 109.9 |
| Wing loading, lb/sq ft . . . . .                           | 19.7  |
| Center-of-gravity position (percent $\bar{c}$ ) . . . . .  | 16.7  |
| Moment of inertia in pitch, slug/ft <sup>2</sup> . . . . . | 3.90  |



3570

NACA RM S151107

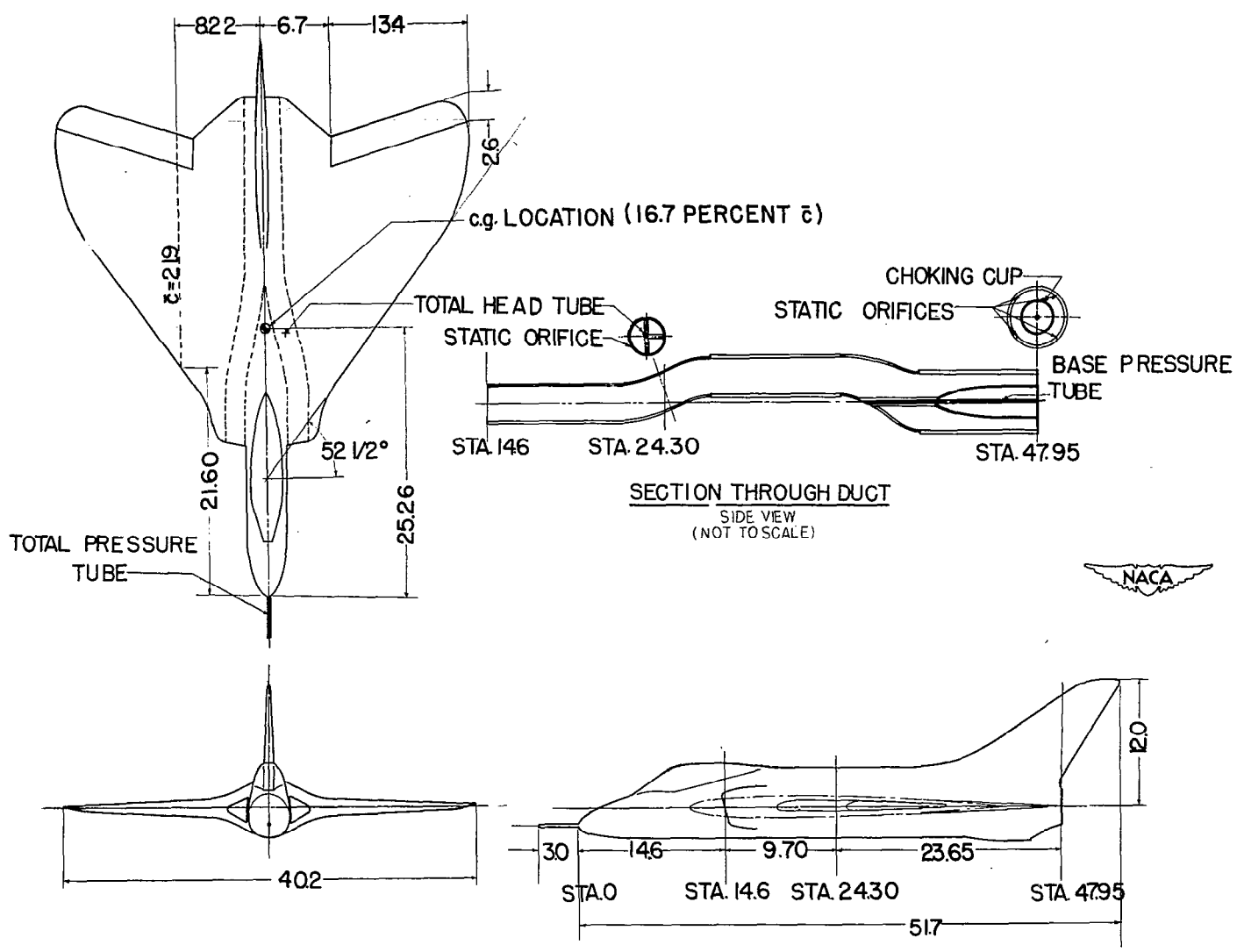
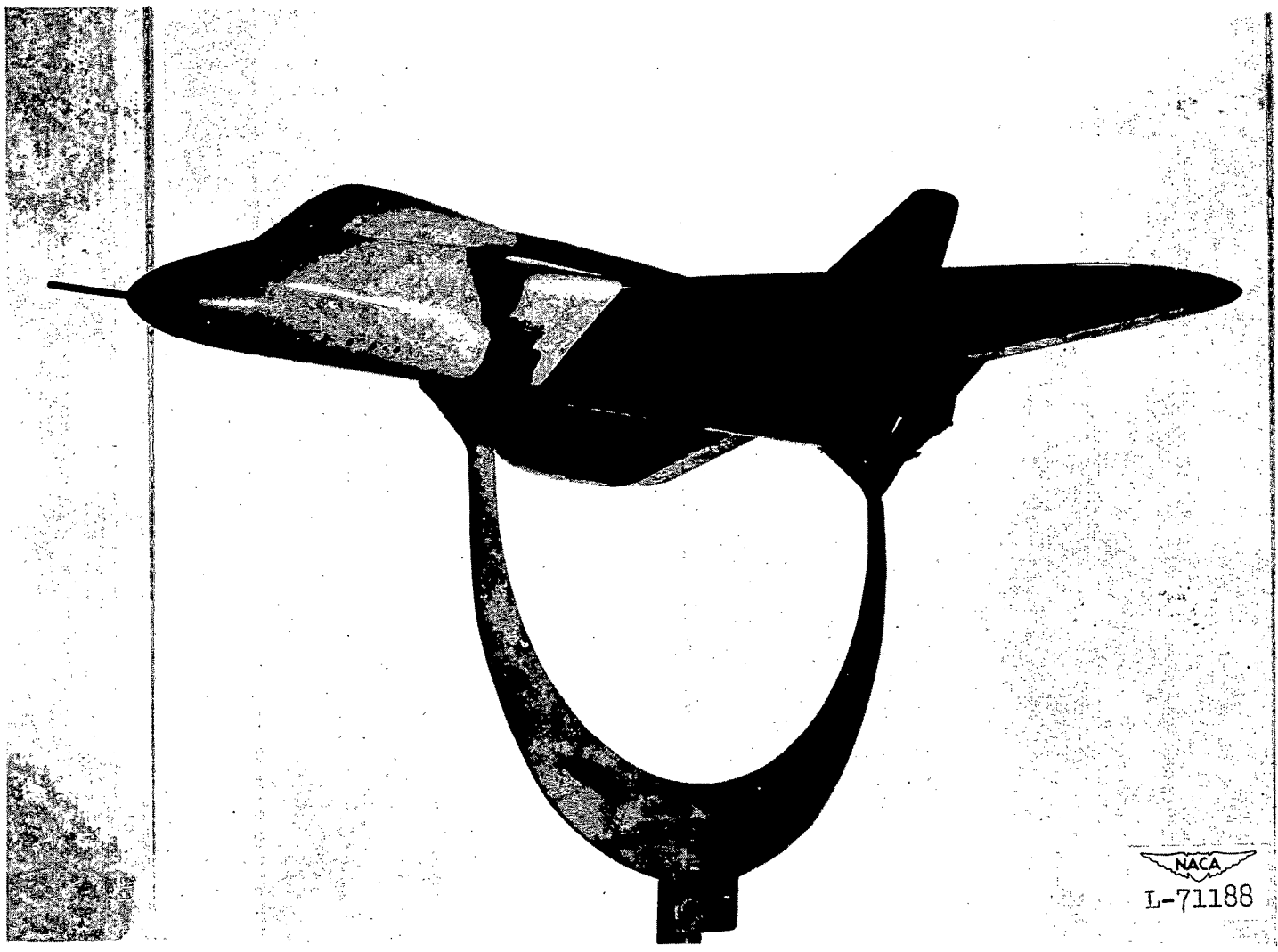


Figure 1.- Three-view drawing of the model; all dimensions are in inches.

3579

NACA RM S151107

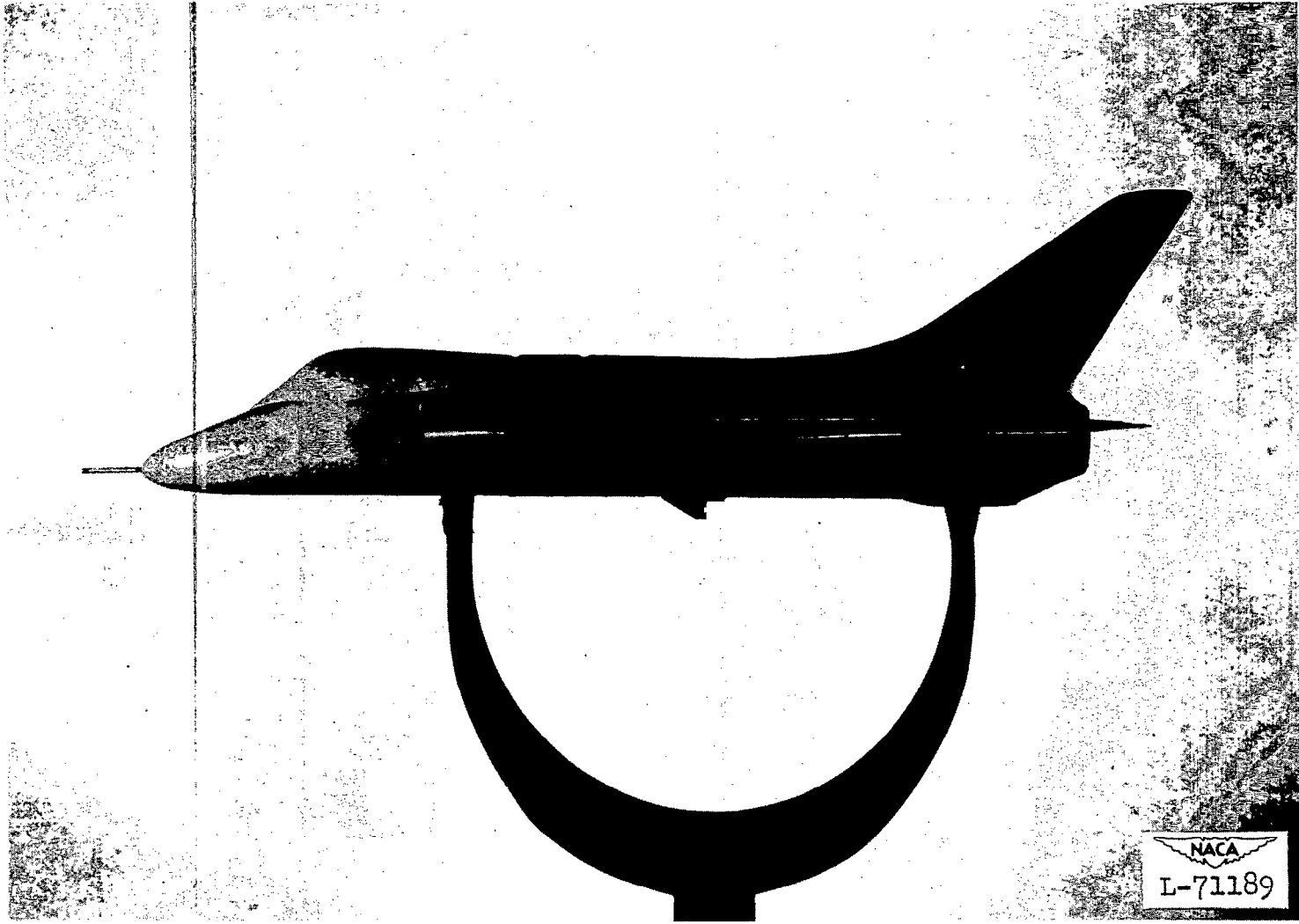


NACA  
L-71188

Figure 2.- Three-quarter front view of the model.

30793

NACA RM SI51107



NACA  
L-71189

Figure 3.- Side view of the model.

30704

NACA RM SL51107

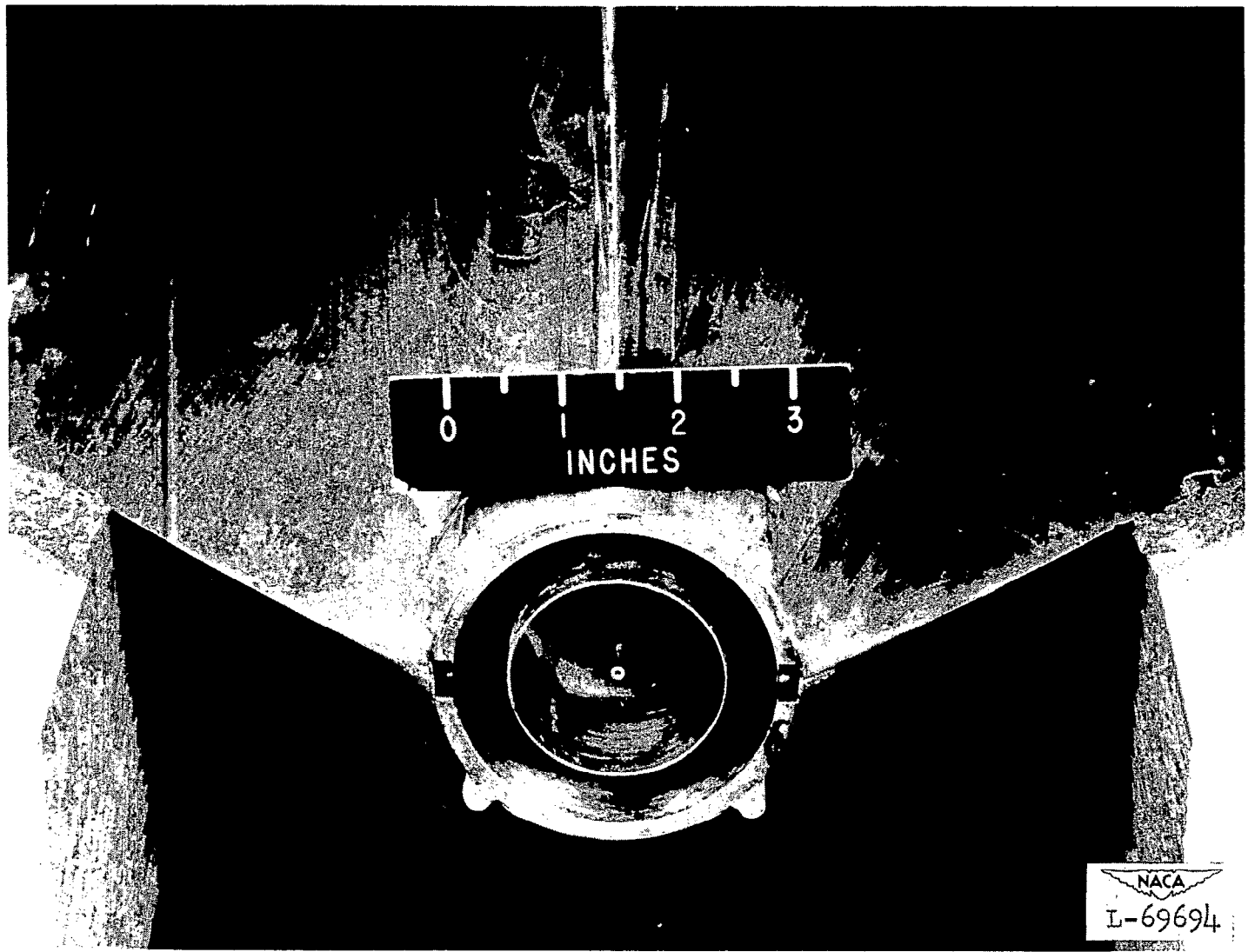
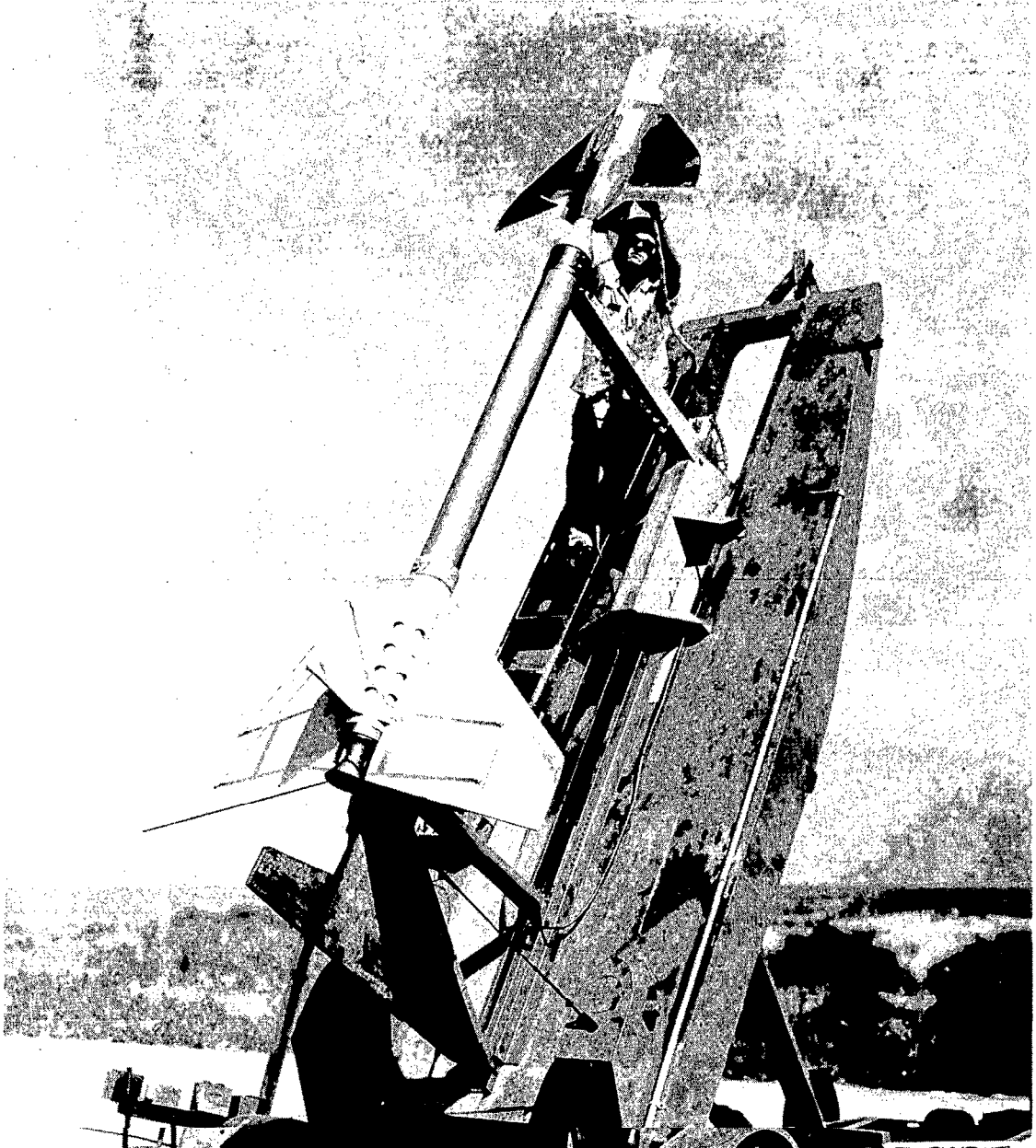


Figure 4.- View showing installation of the choking cup.



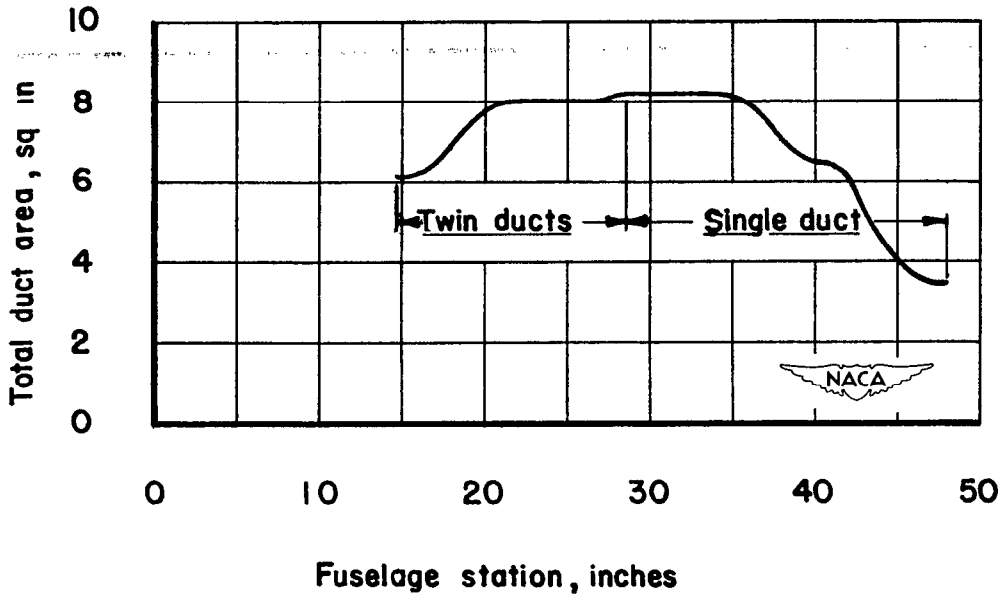


Figure 6.- Duct areas.

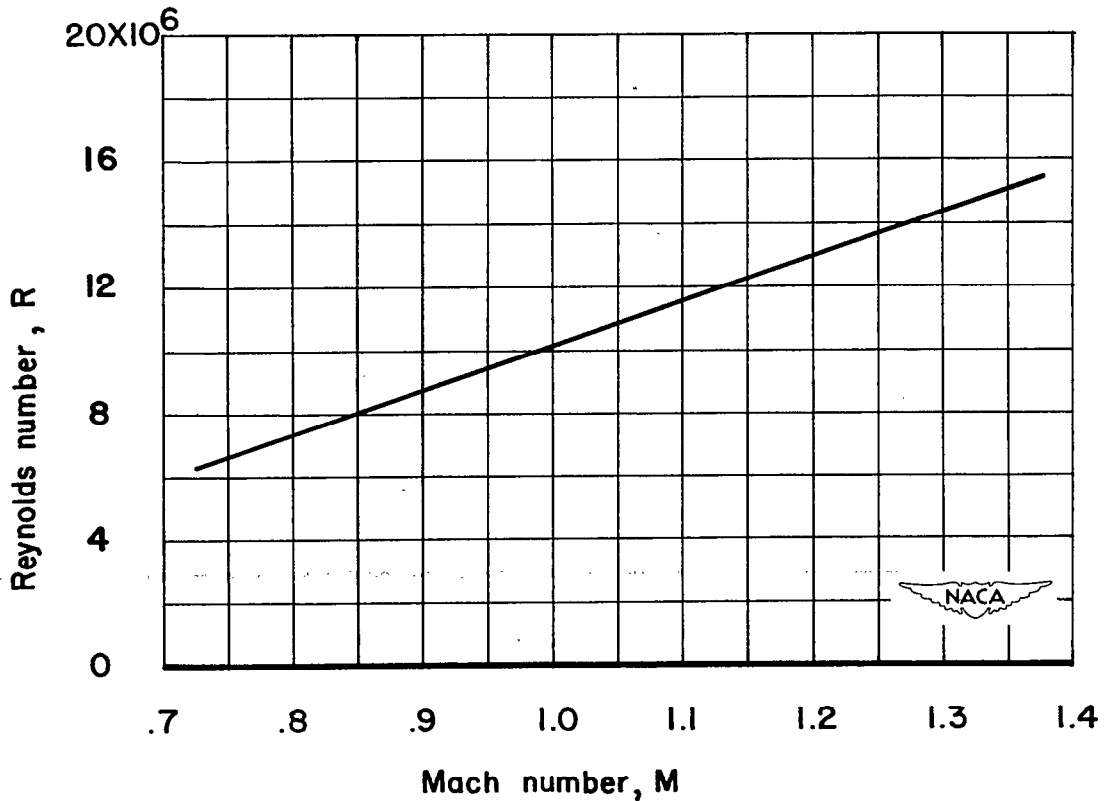


Figure 7.- Reynolds number.

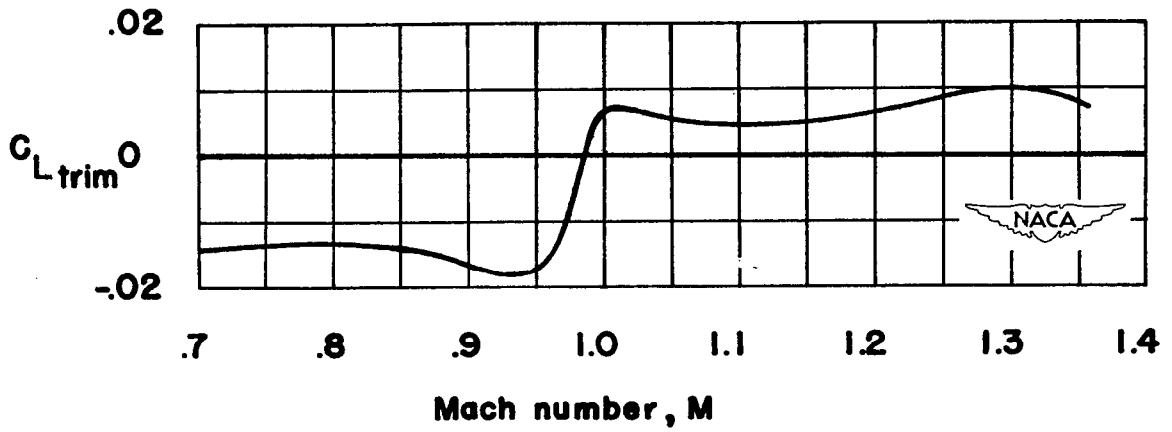


Figure 8.- Trim-lift coefficient.

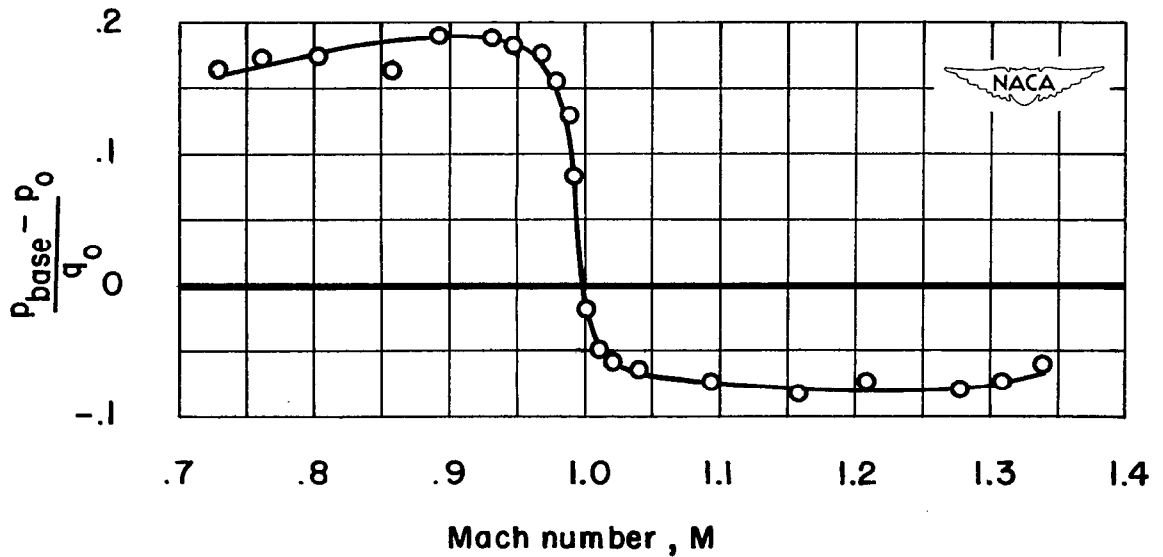


Figure 9.- Pressure coefficient of the choking-cup base.

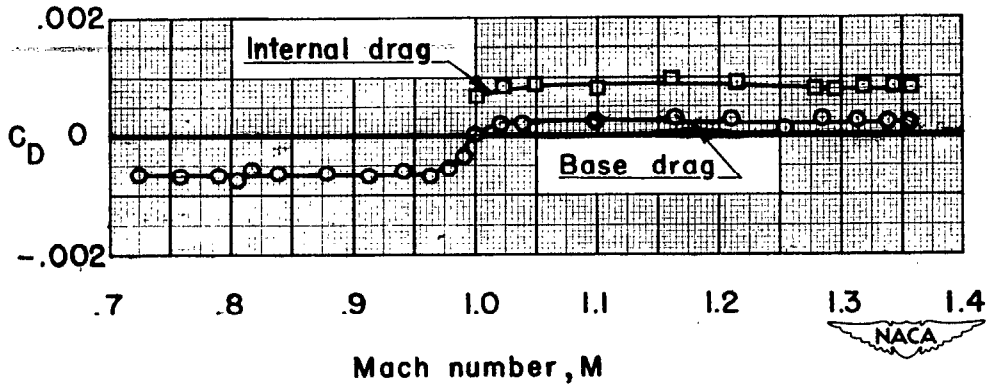


Figure 10.- Internal and base drag.

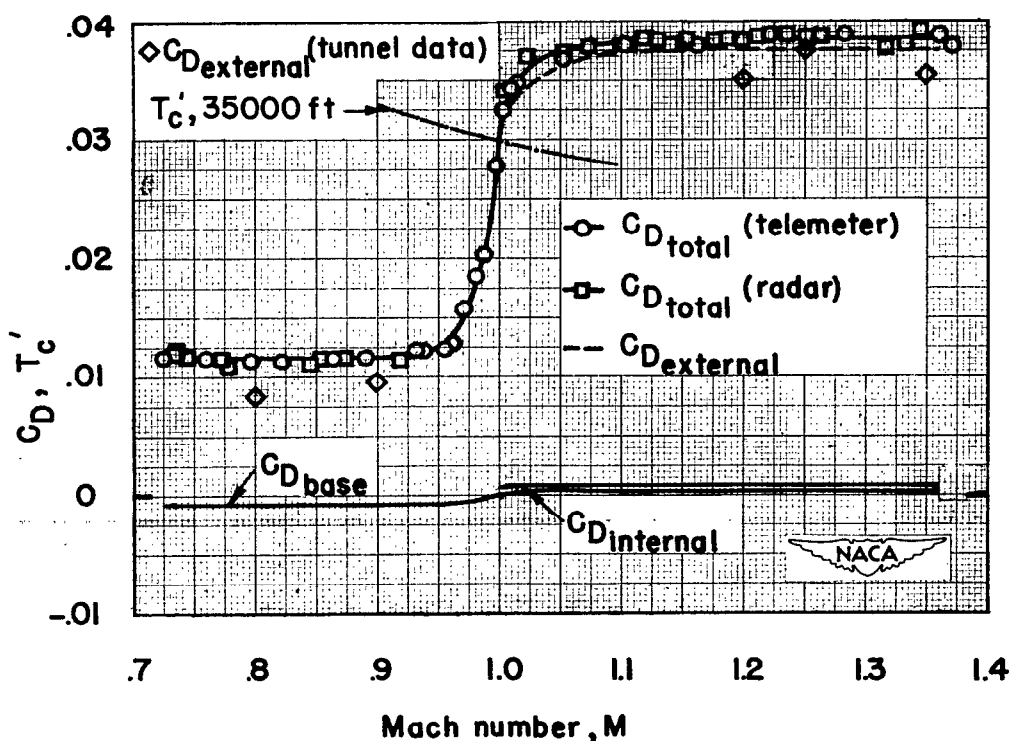
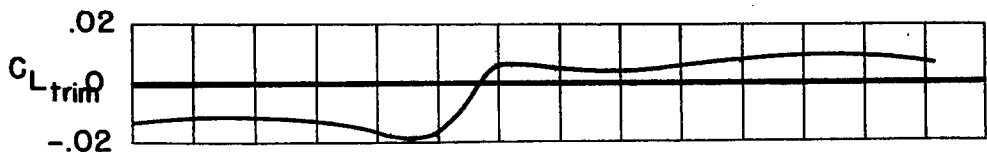


Figure 11.- Lift, drag, and thrust summary.

~~CONFIDENTIAL~~

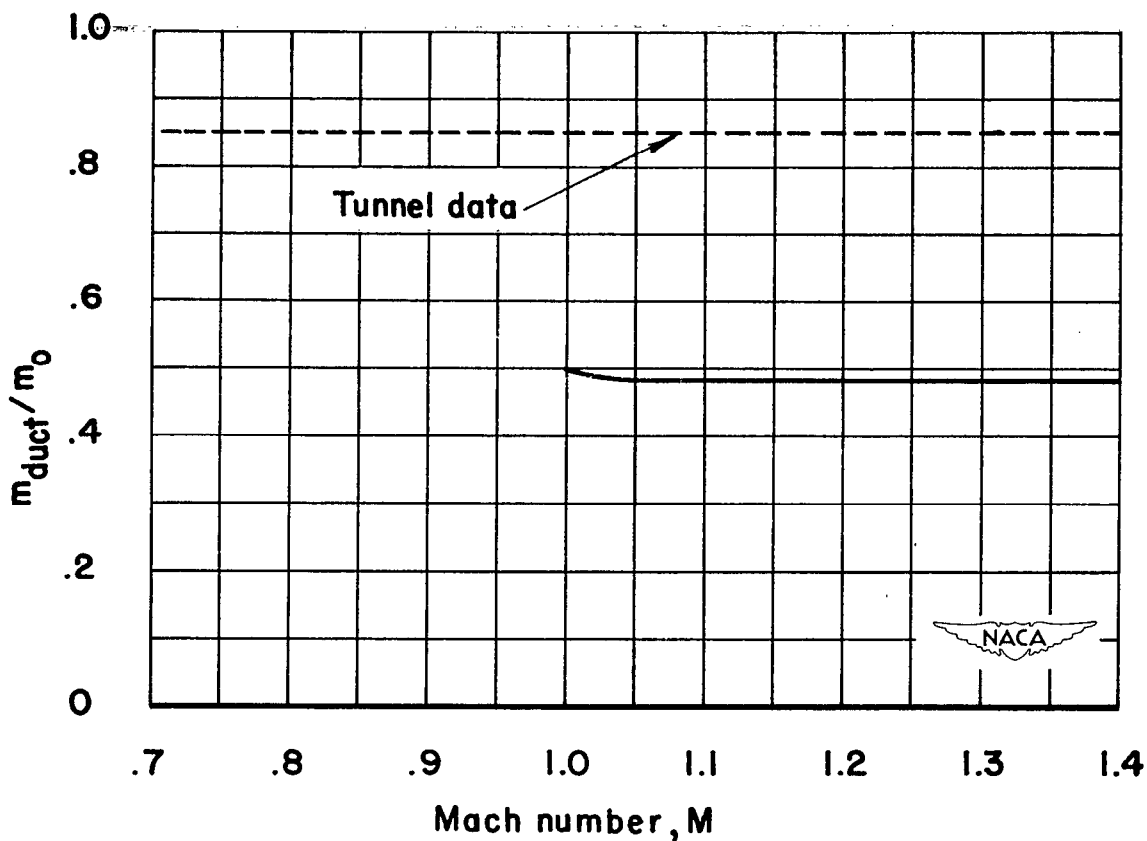


Figure 12.- Mass-flow ratio of the duct.

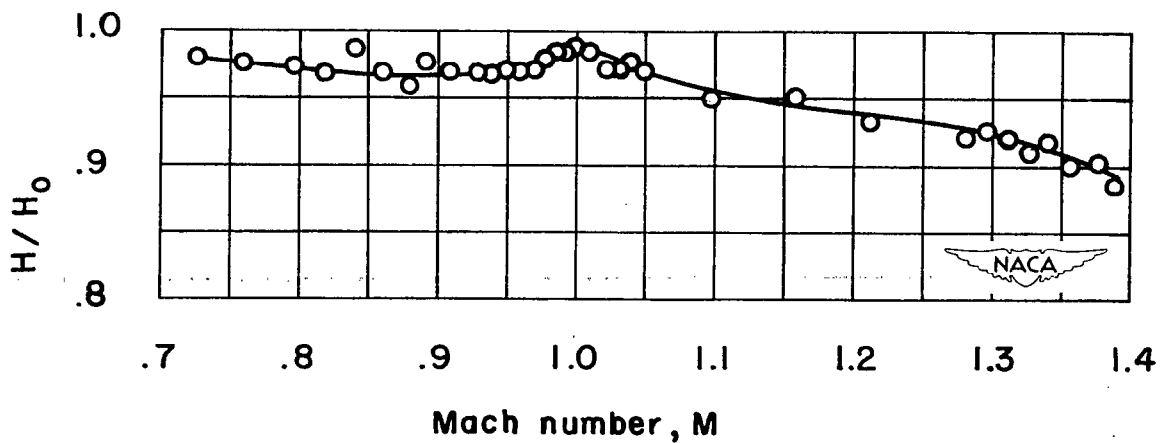


Figure 13.- Total-pressure recovery of the tube located at station 24.30 in the duct.

~~CONFIDENTIAL~~

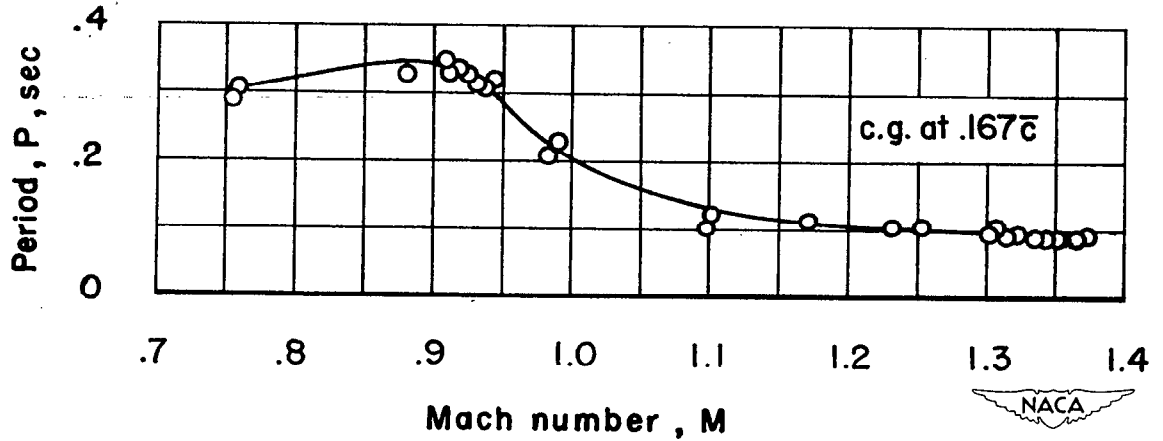


Figure 14.- Period of the short-period longitudinal oscillation.

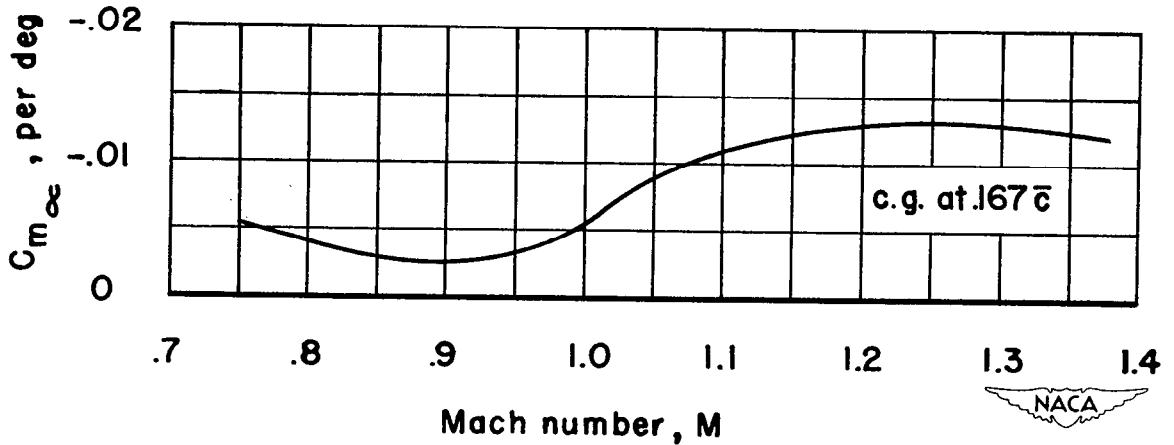


Figure 15.- Rate of change of the pitching-moment coefficient with angle of attack.

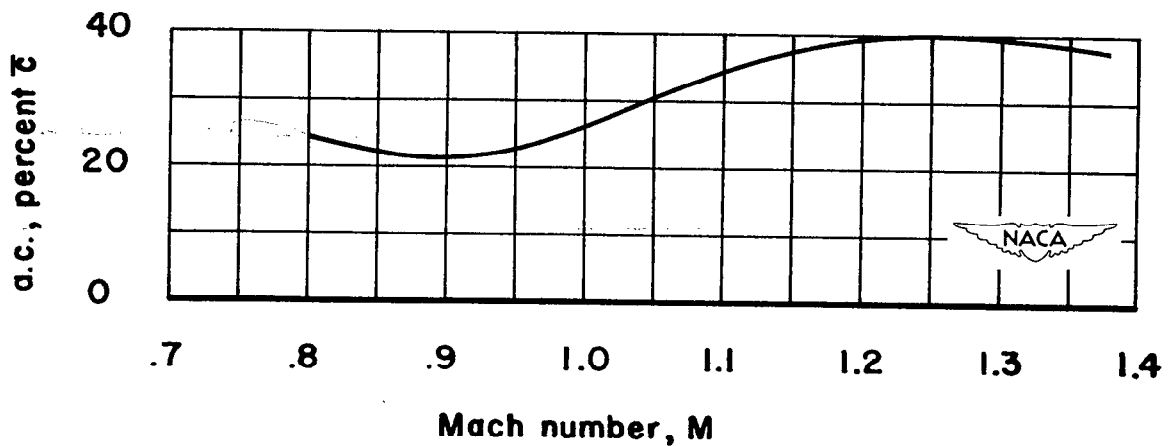


Figure 16.- Aerodynamic center.

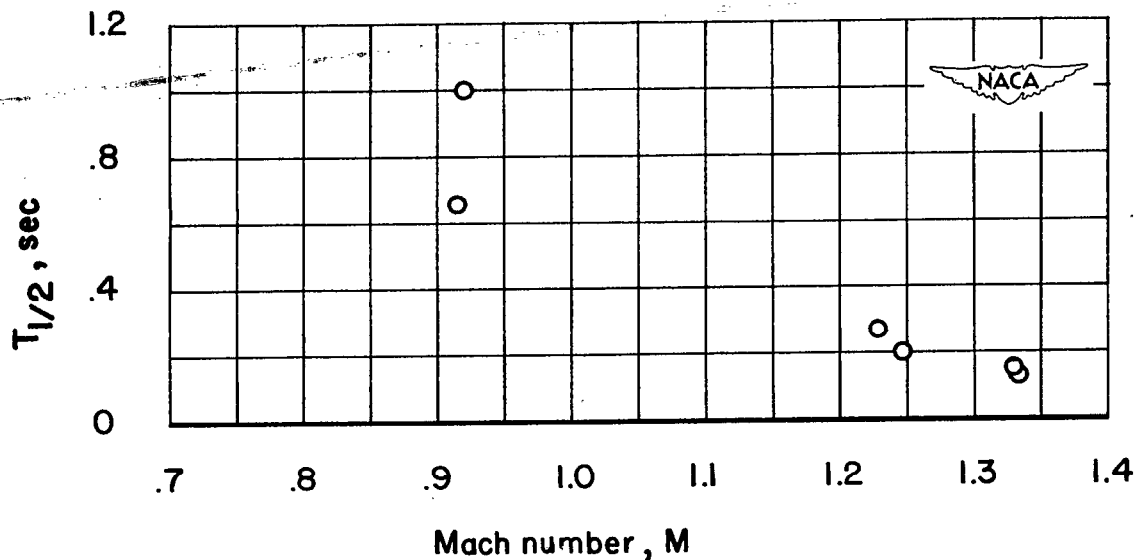


Figure 17.- Time required for the short-period longitudinal oscillation to damp to 1/2 amplitude.

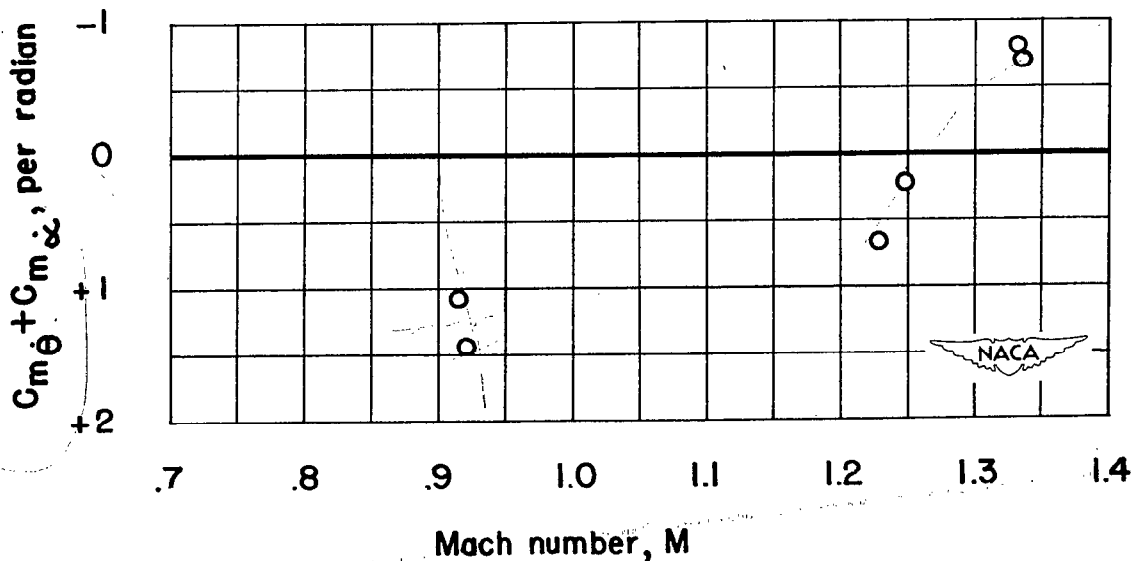


Figure 18.- Total damping factor.

# SECURITY INFORMATION

NASA Technical Library



3 1176 01438 5638

~~CONFIDENTIAL~~